Inorganic Chemistry, Vol. 18, No. 1, 1979 **141**

Contribution from the School of Chemical Sciences,
University of Illinois, Urbana, Illinois 61801

Magnetic-Exchange Interactions in Binuclear Transition-Metal Complexes. 19.[1] Imidazolate- and Biimidazolate-Bridged Copper(II) Complexes. Crystal Structure of μ-Biimidazolato-bis(1,1,4,7,7-pentamethyldiethylenetriamine)dicopper(II) Tetraphenylborate

MUIN S. HADDAD,[2] EILEEN N. DUESLER, and DAVID N. HENDRICKSON*[3]

Received July 7, 1978

The X-ray structure of $[Cu_2(Me_5dien)_2(BiIm)](BPh_4)_2$, where Me_5dien is 1,1,4,7,7-pentamethyldiethylenetriamine and $BiIm^{2-}$ is the 2,2′-biimidazolate dianion, has been determined on a Syntex $P2_1$ diffractometer, by use of 5424 ($F_{obsd} > 2\sigma$) unique reflections, to give final discrepancy indices of $R = 0.048$ and $R_w = 0.063$. The complex crystallizes in the triclinic space group $P\bar{1}$ in a cell having the dimensions $a = 11.265$ (4) Å, $b = 10.234$ (4) Å, $c = 15.999$ (5) Å, $\alpha = 101.78$ (3)°, $\beta = 104.04$ (3)°, and $\gamma = 107.06$ (3)°. The observed and calculated densities are 1.27 (1) and 1.26 g/cm^3, respectively. One formula unit comprises the unit cell with half the binuclear complex in the asymmetric unit. The $BiIm^{2-}$ bridges two distorted, square-pyramidal copper(II) ions having a Cu–Cu distance of 5.489 (1) Å. Variable-temperature magnetic susceptibility data measured down to 4.2 K do not show any magnetic-exchange interaction and consequently $|J| \leq$ ca. 0.5 cm^{-1}. The positioning of each imidazolate ion of the BiIm unit such that it bridges from an equatorial coordination site of one copper(II) ion to the axial coordination site of the second copper(II) ion is proposed as a reason for attenuating the exchange interaction. Binuclear complexes of the general formula $[Cu_2(triamine)_2(Im)](ClO_4)_3$ have also been prepared, and their magnetic susceptibility data indicate antiferromagnetic exchange behavior with J values ranging from −20 to −40 cm^{-1}. The observed trend in the J values is discussed in terms of both the variation of the relative orientation of the bridging imidazolate plane and the copper(II) coordination plane and a change in the copper(II) ground state as indicated by the EPR spectra.

Introduction

The established imidazolate bridge between copper(II) and zinc(II) ions in bovine erythrocyte superoxide dismutase (BESOD),[4] the antiferromagnetic interaction with $J = -26$ cm^{-1} reported for the all copper(II) BESOD,[5] and the imidazolate-bridged heme a_3-Cu(II) model proposed[6] for cytochrome oxidase have precipitated recent work to prepare and characterize simple complexes with imidazolate bridges between copper(II) and iron(III) ions. Reed et al.[7] very recently reported the preparation of some imidazolate-bridged polymeric manganese(II)–porphyrin complexes. An exchange parameter, J, of -8 ± 2 cm^{-1} was determined for this polymeric compound, and this, together with data on copper(II) systems, led Reed et al. to attack Palmer's model[6] for cytochrome oxidase. Palmer, Wilson, et al.[8] have very recently provided more substantial magnetic susceptibility data to support the Palmer model.

Lippard et al.[9-11] have prepared one tetranuclear and three binuclear copper(II) complexes. The copper coordination geometries are square planar or square pyramidal, and it was found that when the imidazolate bridge is coplanar with the (equatorial) plane of the copper complex, there is an antiferromagnetic exchange interaction with $J = -87.4$ cm^{-1}. If the imidazolate bridges from one equatorial site to another but is perpendicular to the plane of the complex, the J is in the range of −27 to −30 cm^{-1}. In a very recent paper,[12] we reported the preparation of some 11 additional binuclear copper(II) complexes with imidazolate and substituted imidazolate bridges. All of the complexes except one have five-coordinate copper(II) ions. It was found that, as the ground state of the copper(II) ions is varied by changing the nonbridging ligands, the exchange parameter varied in the range of 0.5 cm^{-1} $< -J <$ 49 cm^{-1}. The disposition of the imidazolate bridge, that is, whether it bridges between equatorial or axial coordination sites, was also found to be important.

In this paper we report the single-crystal X-ray structure of $[Cu_2(Me_5dien)_2(BiIm)](BPh_4)_2$, where Me_5dien is 1,1,4,7,7-pentamethyldiethylenetriamine and $BiIm^{2-}$ is the dianion of 2,2′-biimidazole. It is shown how the orientation of the substituted imidazolate bridge in this complex leads to a very weak magnetic exchange interaction with $|J| <$ ca. 0.5 cm^{-1}. In addition, the preparation and characterization are reported for four new imidazolate-bridged copper(II) complexes with the composition $[Cu_2(triamine)_2(Im)](ClO_4)_3$, where the triamine is variously Me_5dien (1,1,4,7,7-pentamethyldiethylenetriamine), Et_5dien (1,1,4,7,7-pentaethyldiethylenetriamine), dien (diethylenetriamine), or dpt (dipropylenetriamine).

It is relevant to note that only very recently have binuclear complexes been reported that incorporate a $BiIm^{2-}$ bridge. Rasmussen et al.[13] reported the properties and X-ray structure of $Rh_2(COD)_2(BiIm)$, where COD is 1,5-cyclooctadiene. The structure of tetranuclear $Rh_4(CO)_8(BiIm)_2$ was also reported.[14] Biimidazolate bridging was also reported[15] for $[(\eta^5\text{-}C_5H_5)_2Ti]_2(BiIm)$, a compound that shows an antiferromagnetic interaction with $J = -25.2$ cm^{-1}. The EPR spectra for this last compound proved to be very interesting.

Experimental Section

Compound Preparation. Diethylenetriamine (Union Carbide), dipropylenetriamine (Aldrich), 1,1,4,7,7-pentamethyldiethylenetriamine (Ames Laboratories), 1,1,4,7,7-pentaethyldiethylenetriamine (Ames Laboratories), and imidazole (Aldrich) were used as received. Elemental analyses were performed by the microanalytical laboratory of the School of Chemical Sciences, University of Illinois. The analytical data are compiled in Table I.[16]

The preparation of the compound $[Cu_2(Me_5dien)_2(BiIm)](BPh_4)_2$, where $BiIm^{2-}$ is the dianion of 2,2′-biimidazole, is described in a previous paper.[12] Crystals were grown by a slow evaporation of an acetonitrile solution.

Samples of $[Cu_2(triamine)_2(Im)](ClO_4)_3$, where triamine is variously dien, dpt, Me_5dien, or Et_5dien, were prepared in the following general way. To a methanolic solution (20 mL) of ca. 1.5 g (4 mmol) of $Cu(ClO_4)_2 \cdot 6H_2O$ was added a stoichiometric amount of triamine. To the filtered blue solution was added a methanolic solution (10 mL) of ca. 0.14 g of imidazole (1 mmol) and ca. 0.08 g of NaOH. The resulting solution then acquires a blue-purple color. Cooling the solutions in the refrigerator results in the precipitation of microcrystalline purple products. The hydrated compound $[Cu_2(Me_5dien)_2(Im)](ClO_4)_3 \cdot H_2O$ was obtained by carrying out the reaction in water, followed by subsequent partial evaporation of the aqueous solution. The Et_5dien complex precipitates as the dihydrate from the

0020-1669/79/1318-0141$01.00/0

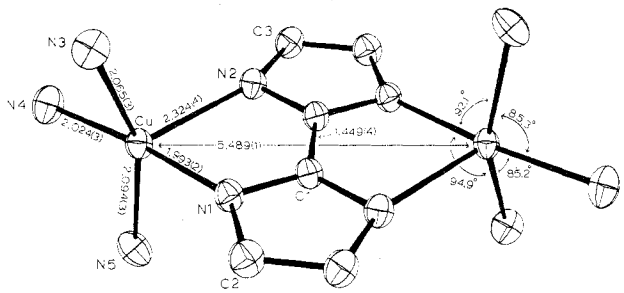

Figure 1. ORTEP plot of the inner coordination about each copper(II) ion and the bridging biimidazolate dianion in $Cu_2(Me_5dien)_2(BiIm)^{2+}$. Thermal ellipsoids for 25% probability are depicted.

methanolic solution. Considerable difficulty was encountered in obtaining a powdered sample of $[Cu_2(Et_5dien)_2(Im)](ClO_4)_3 \cdot 2H_2O$, for in many preparations the product separated as a "gummy" material. All compounds were washed with ether and dried in a vacuum desiccator over P_4O_{10}.

Physical Measurements. Variable-temperature (4.2–286 K) magnetic susceptibility data were obtained with a Princeton Applied Research Model 150A vibrating-sample magnetometer operating at 12.7 kG and calibrated with $CuSO_4 \cdot 5H_2O$ as described in a previous paper.[17] All data were corrected for diamagnetism[18] and TIP (taken as 120×10^{-6} cgsu/mol of binuclear complex). All least-squares fittings were performed using a new version of the minimization computer program STEPT.[19]

EPR spectra of powdered samples were recorded on a Varian E-9 X-band spectrometer and a Varian E-15 Q-band spectrometer as described previously.[12]

Crystal Measurements. A dark purple crystal of $[Cu_2(Me_5dien)_2(BiIm)](BPh_4)_2$ with dimensions of $0.3 \times 0.3 \times 0.4$ mm was used for data collection. Preliminary examination of the crystal and data collection were performed on a Syntex $P2_1$ four-circle automatic diffractometer equipped with a graphite monochromator. The cell dimensions (see Table II) were obtained by a least-squares fit to the automatically centered settings for 15 reflections.[20] The space group $P\bar{1}$ was assumed to be the correct one on the basis of the density. Subsequent refinements were done in this space group. Three standard reflections from different parts of reciprocal space were monitored every 57 reflections as a check on the crystal and electronic stability, and no significant change in the counting statistics was found. Lorentz and polarization corrections were applied to the data. Absorption corrections were deemed unnecessary in view of the small linear absorption coefficient. Additional details relating to the measurement of data are given in Table II.

Structure Solution and Refinement. A three-dimensional Patterson map was calculated with use of the 5424 observed reflections, and the copper atom position was readily calculated. A structure factor calculation for the copper atom position gave an agreement factor of $R = 0.48$. The copper atom position was used to generate a Fourier map. The scattering factor tables for neutral atoms were taken from the analytical expression used in ref 21. The effects of anomalous dispersion for the copper atom were included in the calculated structure factors by use of the real and imaginary dispersion corrections of Cromer and Liberman.[22]

From the Fourier map generated with the use of only the copper position, it was possible to locate 38 nonhydrogen atoms in the asymmetric unit. With the 38 located atom positions another Fourier map yielded the remainder of the 43 nonhydrogen atom positions. Six cycles of block-diagonal least-squares refinements on these 43 positions with isotropic thermal parameters dropped the R factor to 0.101. Two cycles of block refinement employing anisotropic thermal parameters reduced R to 0.074. The function minimized was $\sum w||F_o| - |F_c||^2$, where $w = 1/(\sigma(F_o) + 0.04F_o^2)^2$ and $\sigma(F_o) = \sigma(I)/2|F_o|(Lp)$ where Lp is the Lorentz–polarization factor. At this point, a difference Fourier map was generated which yielded 35 hydrogen atom positions from the top 40 peaks. The remaining hydrogen atom positions were calculated. The BPh_4^- hydrogen atom positions were calculated at this point with the assumption of a C–H bond distance of 1.0 Å. All hydrogen atoms were assigned the last isotropic thermal parameter of the carbon atom to which they are bonded. The final full-matrix least-squares refinements reached convergence with $R = 0.048$ and $R_w = 0.063$, where

$$R = \sum||F_o| - |F_c||/\sum|F_o|$$

$$R_w = [\sum w||F_o| - |F_c||^2/\sum w|F_o|^2]^{1/2}$$

The expected error in a measurement of unit weight (erf) is defined by $[\sum w(|F_o| - |F_c|)^2/(m-n)]^{1/2}$, where m is the number of reflections and n is the number of variables. The final erf value is 1.15. A final difference map showed the four highest peaks (0.37–0.57 of a hydrogen atom) were within 1.05 Å of the copper atom position. A compilation of the final values of $|F_o|$ and $|F_c|$ for the complete 7565 reflection data set obtained in the last refinement cycle is available.[16]

Table II. Experimental Data for the X-ray Diffraction Study of $[Cu_2(Me_5dien)_2(BiIm)](BPh_4)_2$

Crystal Parameters	
$a = 11.265$ (4) Å	space group: $P\bar{1}$
$b = 10.234$ (4) Å	$Z = 1$ (1 binuclear complex)
$c = 15.999$ (5) Å	mol wt 1244.29
$\alpha = 101.78$ (3)°	ρ(calcd) = 1.26 g cm^{-3}
$\beta = 104.04$ (3)°	ρ(calcd) = 1.27 (1) g cm^{-3} (flotation in toluene-*o*-bromotoluene)
$\gamma = 107.06$ (3)°	$V = 1633.5$ Å^3

Measurement of Intensity Data	
radiation:	Mo Kα, λ 0.709 26 Å
monochromator:	graphite cryst
takeoff angle:	6.2°
X-ray beam collimator diameter:	1.0 mm
cryst orientation:	random
reflections measured:	$(h, \pm k, \pm l)$
max 2θ:	55°
scan type:	θ–2θ scan technique
scan speed:	variable, 2.0–15.0° min^{-1}
base width:	2.2° in 2θ
bkgd measurement:	stationary crystal, stationary counter; $R = 0.3^a$
reflections collected:	7565 unique reflections; 5424 observed above $2\sigma(I)$ level
abs coeff:	7.3 cm^{-1}

[a] R is ratio of scan time to background counting time.

Results and Discussion

Molecular Structure of $[Cu_2(Me_5dien)_2(BiIm)](BPh_4)_2$. The single-crystal structure of $[Cu_2(Me_5dien)_2(BiIm)](BPh_4)_2$ was solved using standard heavy-atom techniques. The final positional and anisotropic thermal parameters are presented in Tables III and IV, respectively, while the bond distances and angles are given in Table V.

The structure consists of discrete binuclear cations, $Cu(Me_5dien)_2(BiIm)^{2+}$, and BPh_4^- anions. The binuclear cation is located about a crystallographic center of inversion. In Figure 1 is shown a perspective view of the inner coordination about each copper(II) ion and the bridging biimidazolate dianion. Figure 2 gives a stereoscopic view of the binuclear

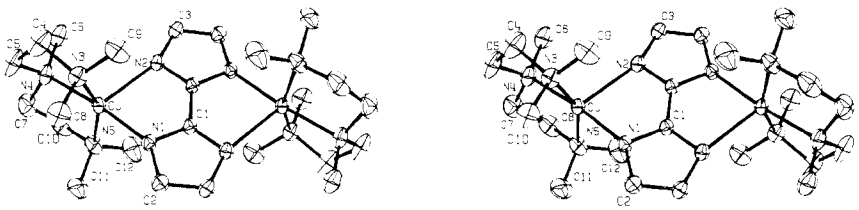

Figure 2. Stereoscopic view of $Cu_2(Me_5dien)_2(BiIm)^{2+}$. Hydrogen atoms are not shown.

Table III. Final Positional Parameters[a] for $[Cu_2(Me_5dien)_2(BiIm)](BPh_4)_2$ Including Hydrogen Atoms[b]

atom	x	y	z	atom	x	y	z
Cu	0.03134 (3)	0.19453 (4)	0.15731 (2)	H(3)	0.255 (3)	−0.039 (3)	0.174 (2)
N(1)	−0.0832 (2)	0.1228 (3)	0.0288 (2)	H(4A)	−0.014 (4)	0.052 (5)	0.312 (3)
N(2)	0.1148 (2)	0.0214 (3)	0.1087 (2)	H(4B)	−0.119 (4)	0.095 (4)	0.334 (3)
N(3)	−0.1125 (3)	0.0908 (3)	0.2051 (2)	H(5A)	0.088 (4)	0.200 (5)	0.403 (3)
N(4)	0.1418 (3)	0.2850 (4)	0.2889 (2)	H(5B)	−0.000 (4)	0.340 (5)	0.337 (3)
N(5)	0.1581 (3)	0.3709 (3)	0.1362 (2)	H(6A)	0.287 (4)	0.261 (4)	0.380 (3)
C(1)	−0.0501 (3)	0.0250 (3)	−0.0210 (2)	H(6B)	0.302 (4)	0.230 (4)	0.282 (3)
C(2)	−0.1794 (3)	0.1415 (4)	−0.0344 (2)	H(6C)	0.194 (4)	0.124 (5)	0.311 (3)
C(3)	0.1983 (3)	−0.0550 (4)	0.1166 (2)	H(7A)	0.149 (4)	0.488 (5)	0.302 (3)
C(4)	−0.0508 (5)	0.1210 (7)	0.3037 (3)	H(7B)	0.278 (5)	0.470 (5)	0.349 (3)
C(5)	0.0507 (5)	0.2698 (7)	0.3416 (3)	H(8A)	0.305 (4)	0.540 (5)	0.226 (3)
C(6)	0.2375 (5)	0.2159 (6)	0.3170 (3)	H(8B)	0.336 (4)	0.396 (4)	0.229 (3)
C(7)	0.2144 (5)	0.4381 (5)	0.2986 (4)	H(9A)	−0.235 (4)	−0.122 (5)	0.183 (3)
C(8)	0.2666 (5)	0.4460 (5)	0.2225 (4)	H(9B)	−0.092 (4)	−0.105 (4)	0.174 (3)
C(9)	−0.1684 (5)	−0.0650 (5)	0.1620 (4)	H(9C)	−0.210 (5)	−0.093 (5)	0.105 (3)
C(10)	−0.2181 (4)	0.1510 (6)	0.1898 (4)	H(10A)	−0.177 (4)	0.260 (4)	0.217 (3)
C(11)	0.0814 (6)	0.4615 (5)	0.1116 (4)	H(10B)	−0.253 (4)	0.135 (4)	0.124 (3)
C(12)	0.2154 (6)	0.3326 (6)	0.0645 (5)	H(10C)	−0.283 (4)	0.110 (4)	0.215 (3)
B	0.7093 (3)	0.5867 (4)	0.2995 (2)	H(11A)	0.139 (4)	0.544 (5)	0.107 (3)
C(13)	0.8651 (3)	0.6862 (3)	0.3193 (2)	H(11B)	0.007 (4)	0.405 (5)	0.051 (3)
C(14)	0.9335 (3)	0.7943 (4)	0.4008 (2)	H(11C)	0.039 (4)	0.472 (5)	0.155 (3)
C(15)	1.0666 (4)	0.8786 (4)	0.4259 (3)	H(12A)	0.140 (5)	0.296 (5)	0.006 (3)
C(16)	1.1347 (3)	0.8592 (4)	0.3671 (3)	H(12B)	0.270 (4)	0.268 (5)	0.085 (3)
C(17)	1.0723 (4)	0.7547 (4)	0.2857 (3)	H(12C)	0.262 (5)	0.418 (5)	0.061 (3)
C(18)	0.9400 (3)	0.6692 (4)	0.2625 (3)	H(14)	0.885 (0)	0.813 (0)	0.444 (0)
C(19)	0.6423 (3)	0.4629 (3)	0.2004 (2)	H(15)	1.112 (0)	0.952 (0)	0.486 (0)
C(20)	0.5677 (3)	0.3209 (3)	0.1895 (2)	H(16)	1.229 (0)	0.921 (0)	0.383 (0)
C(21)	0.5087 (3)	0.2164 (4)	0.1067 (3)	H(17)	1.122 (0)	0.739 (0)	0.243 (0)
C(22)	0.5214 (3)	0.2481 (4)	0.0290 (2)	H(18)	0.897 (0)	0.593 (0)	0.203 (0)
C(23)	0.5927 (4)	0.3863 (5)	0.0357 (2)	H(20)	0.556 (0)	0.293 (0)	0.244 (0)
C(24)	0.6517 (4)	0.4909 (4)	0.1192 (2)	H(21)	0.456 (0)	0.117 (0)	0.103 (0)
C(25)	0.7087 (3)	0.5023 (3)	0.3770 (2)	H(22)	0.480 (0)	0.173 (0)	−0.031 (0)
C(26)	0.8100 (3)	0.4547 (4)	0.4091 (2)	H(23)	0.602 (0)	0.412 (0)	−0.020 (0)
C(27)	0.8020 (4)	0.3631 (4)	0.4627 (2)	H(24)	0.703 (0)	0.590 (0)	0.122 (0)
C(28)	0.6924 (4)	0.3170 (4)	0.4873 (2)	H(26)	0.892 (0)	0.488 (0)	0.393 (0)
C(29)	0.5912 (3)	0.3643 (4)	0.4595 (2)	H(27)	0.877 (0)	0.331 (0)	0.483 (0)
C(30)	0.5998 (3)	0.4560 (4)	0.4060 (2)	H(28)	0.686 (0)	0.250 (0)	0.525 (0)
C(31)	0.6269 (3)	0.6969 (3)	0.3073 (2)	H(29)	0.511 (0)	0.333 (0)	0.478 (0)
C(32)	0.5573 (3)	0.7254 (4)	0.2322 (2)	H(30)	0.526 (0)	0.490 (0)	0.388 (0)
C(33)	0.4965 (4)	0.8255 (4)	0.2397 (3)	H(32)	0.551 (0)	0.671 (0)	0.171 (0)
C(34)	0.5018 (4)	0.9019 (5)	0.3225 (3)	H(33)	0.448 (0)	0.842 (0)	0.184 (0)
C(35)	0.5663 (4)	0.8742 (5)	0.3986 (3)	H(34)	0.460 (0)	0.976 (0)	0.327 (0)
C(36)	0.6277 (4)	0.7748 (4)	0.3908 (2)	H(35)	0.569 (0)	0.926 (0)	0.460 (0)
H(2)	−0.218 (3)	0.207 (4)	−0.021 (2)	H(36)	0.674 (0)	0.758 (0)	0.447 (0)

[a] Standard deviations of the least significant figures are given in parentheses and are given in this fashion in succeeding tables. [b] The hydrogen atoms in $[Cu_2(Me_5dien)_2(BiIm)]^{2+}$ were located in the Fourier map. The hydrogen atom positions for the BPh_4^- anions were calculated with fixed bond lengths of 1.0 Å.

cation with the cation atom numbering scheme indicated.

Table VI shows that the $BiIm^{2-}$ bridge is planar as it is in $Rh_2(COD)_2(BiIm)$.[13] The central C–C distance (i.e., C(1)–C(1)′ = 1.449 (4) Å) in $Cu_2(Me_5dien)_2(BiIm)^{2+}$ is larger than that observed (1.405 (12) Å) for the binuclear rhodium complex. The other $BiIm^{2-}$ bond distances and angles are the same within experimental error for the two complexes. The molecular dimensions for the $BiIm^{2-}$ bridge in $[Cu(Me_5dien)_2(BiIm)](BPh_4)_2$ can be compared with the imidazolate bridge in the polymeric copper(II) complex Cu(Im)(ImH)Cl.[23] Using the atom numbering scheme as found in Figure 2, we observed that the C(1)–N(1) and C(1)–N(2) distances compare with C–N distances of 1.329 (9) and 1.333 (9) Å for the polymer. The polymeric complex distances that are comparable to N(2)–C(3) and N(1)–C(2) are 1.360 (10) and 1.402 (12) Å, which, considering the relatively large esd's for the polymer structure, are essentially the same as those found for $[Cu_2(Me_5dien)_2(BiIm)](BPh_4)_2$ (see Figure 1). Finally, the C(2)–C(3)′ distance in the imidazolate bridge of the polymer is 1.365 (11) Å, which compares favorably with the C(2)–C(3)′ = 1.355 (5) Å dimension in the present structure. It appears, then, that the imidazolate moieties found in the $BiIm^{2-}$ bridge of $Cu_2(Me_5dien)_2(BiIm)^{2+}$ are structured the same as the imidazolate bridge in Cu(Im)(ImH)Cl.

The stereoscopic plot of $Cu_2(Me_5dien)_2(BiIm)^{2+}$ illustrated in Figure 2 can be used to obtain the best view of the coordination geometry about the copper(II) ion. It is possible to view the coordination geometry as being either distorted from trigonal bipyramidal, where the trigonal plane consists of the atoms N(2), N(3), and N(5), or distorted from square pyramidal, where the basal plane consists of the atoms N(1), N(3), N(4), and N(5). Least-squares-fit planes and deviations of atoms from the planes are given in Table VI. As has been mentioned before,[24,25] the degree of distortion of the copper coordination geometry away from either of the limiting structures can be judged by the value of the angle between the two primary nitrogen atoms of Me_5dien and the copper atom, N(3)–Cu–N(5) in the present structure. For the TBP case this angle would be 120° whereas, for the SP case the angle would be 180°. In this $BiIm^{2-}$ compound this angle is 155.70 (13)°, which is close to the corresponding angles in $[Cu_2(Me_5dien)_2(N_3)_2](BPh_4)_2$ (153.1 (2)°)[25] and $[Cu_2(Me_5dien)_2(CA)](BPh_4)_2$ (151.8 (2)°),[24] where CA^{2-} is the dianion of chloranilic acid.

The EPR data (vide infra) for $[Cu_2(Me_5dien)_2(BiIm)](BPh_4)_2$ clearly indicate that the electronic ground state is closest to square pyramidal, i.e., $d_{x^2-y^2}$. The *xy* plane is probably the same as the plane determined by atoms N(1),

Table IV. Anisotropic Thermal Parameters[a] for $[Cu_2(Me_5dien)_2(BiIm)](BPh_4)_2$

atom	B_{11}	B_{22}	B_{33}	B_{12}	B_{13}	B_{23}
Cu	0.00690 (4)	0.00878 (5)	0.00339 (2)	0.00309 (3)	0.00161 (2)	0.00106 (2)
N(1)	0.0077 (2)	0.0093 (3)	0.0037 (1)	0.0048 (2)	0.0018 (1)	0.0016 (2)
N(2)	0.0070 (2)	0.0106 (3)	0.0036 (1)	0.0042 (2)	0.0016 (1)	0.0018 (2)
N(3)	0.0084 (3)	0.0160 (4)	0.0052 (1)	0.0064 (3)	0.0033 (2)	0.0042 (2)
N(4)	0.0112 (3)	0.0163 (5)	0.0039 (1)	0.0061 (3)	0.0010 (2)	0.0003 (2)
N(5)	0.0112 (3)	0.0094 (3)	0.0071 (2)	0.0028 (3)	0.0039 (2)	0.0019 (2)
C(1)	0.0065 (3)	0.0087 (3)	0.0035 (1)	0.0038 (2)	0.0018 (2)	0.0017 (2)
C(2)	0.0092 (3)	0.0126 (4)	0.0048 (2)	0.0070 (3)	0.0022 (2)	0.0029 (2)
C(3)	0.0082 (3)	0.0135 (4)	0.0039 (2)	0.0056 (3)	0.0013 (2)	0.0030 (2)
C(4)	0.0143 (6)	0.0333 (12)	0.0060 (2)	0.0116 (7)	0.0052 (3)	0.0084 (5)
C(5)	0.0164 (6)	0.0334 (12)	0.0034 (2)	0.0111 (7)	0.0029 (3)	0.0016 (4)
C(6)	0.0121 (5)	0.0221 (8)	0.0050 (2)	0.0072 (5)	0.0004 (3)	0.0019 (4)
C(7)	0.0146 (6)	0.0158 (7)	0.0070 (3)	0.0035 (5)	−0.0013 (3)	−0.0031 (4)
C(8)	0.0117 (5)	0.0115 (5)	0.0113 (4)	0.0001 (4)	0.0026 (4)	0.0017 (4)
C(9)	0.0119 (5)	0.0151 (6)	0.0108 (4)	0.0037 (5)	0.0060 (4)	0.0063 (4)
C(10)	0.0114 (5)	0.0238 (8)	0.0077 (3)	0.0109 (5)	0.0055 (3)	0.0063 (4)
C(11)	0.0202 (8)	0.0101 (5)	0.0094 (4)	0.0054 (5)	0.0039 (4)	0.0039 (4)
C(12)	0.0215 (8)	0.0159 (7)	0.0126 (5)	0.0042 (6)	0.0121 (5)	0.0054 (5)
B	0.0072 (3)	0.0098 (4)	0.0034 (1)	0.0037 (3)	0.0020 (2)	0.0019 (2)
C(13)	0.0077 (3)	0.0091 (3)	0.0043 (2)	0.0039 (3)	0.0019 (2)	0.0023 (2)
C(14)	0.0098 (4)	0.00119 (4)	0.0048 (2)	0.0038 (3)	0.0023 (2)	0.0022 (2)
C(15)	0.0096 (4)	0.0105 (4)	0.0065 (2)	0.0023 (3)	0.0012 (2)	0.0019 (2)
C(16)	0.0078 (3)	0.0108 (4)	0.0088 (3)	0.0030 (3)	0.0024 (3)	0.0040 (3)
C(17)	0.0094 (4)	0.0153 (5)	0.0085 (3)	0.0048 (4)	0.0051 (3)	0.0037 (3)
C(18)	0.0099 (4)	0.0120 (4)	0.0058 (2)	0.0041 (3)	0.0033 (2)	0.0015 (2)
C(19)	0.0072 (3)	0.0111 (4)	0.0037 (1)	0.0044 (3)	0.0018 (2)	0.0021 (2)
C(20)	0.0084 (3)	0.0110 (4)	0.0042 (2)	0.0037 (3)	0.0019 (2)	0.0020 (2)
C(21)	0.0082 (3)	0.0119 (4)	0.0060 (2)	0.0023 (3)	0.0018 (2)	0.0008 (2)
C(22)	0.0092 (4)	0.0161 (6)	0.0043 (2)	0.0039 (4)	0.0012 (2)	−0.0004 (2)
C(23)	0.0127 (4)	0.0188 (6)	0.0036 (2)	0.0050 (4)	0.0021 (2)	0.0024 (3)
C(24)	0.0121 (4)	0.0126 (4)	0.0040 (2)	0.0045 (4)	0.0022 (2)	0.0023 (2)
C(25)	0.0079 (3)	0.0099 (4)	0.0030 (1)	0.0036 (3)	0.0015 (2)	0.0012 (2)
C(26)	0.0091 (3)	0.0116 (4)	0.0045 (2)	0.0051 (3)	0.0022 (2)	0.0021 (2)
C(27)	0.0120 (4)	0.0127 (5)	0.0049 (2)	0.0071 (4)	0.0017 (2)	0.0030 (2)
C(28)	0.0134 (4)	0.0120 (4)	0.0041 (2)	0.0047 (4)	0.0020 (2)	0.0028 (2)
C(29)	0.0105 (4)	0.0153 (5)	0.0042 (2)	0.0034 (4)	0.0024 (2)	0.0034 (2)
C(30)	0.0077 (3)	0.0159 (5)	0.0040 (2)	0.0049 (3)	0.0018 (2)	0.0033 (2)
C(31)	0.0063 (3)	0.0102 (4)	0.0044 (2)	0.0032 (3)	0.0019 (2)	0.0019 (2)
C(32)	0.0091 (3)	0.0121 (4)	0.0050 (2)	0.0047 (3)	0.0026 (2)	0.0035 (2)
C(33)	0.0111 (4)	0.0157 (5)	0.0076 (3)	0.0073 (3)	0.0031 (3)	0.0060 (3)
C(34)	0.0132 (5)	0.0165 (6)	0.0094 (3)	0.0101 (5)	0.0046 (3)	0.0051 (4)
C(35)	0.0154 (5)	0.0174 (6)	0.0069 (2)	0.0099 (5)	0.0042 (3)	0.0014 (3)
C(36)	0.0121 (4)	0.0158 (5)	0.0047 (2)	0.0080 (4)	0.0025 (2)	0.0023 (2)

atom	B, Å^2	atom	B, Å^2	atom	B, Å^2	atom	B, Å^2
H(2)	3.8 (0)	H(8B)	6.3 (0)	H(12B)	7.0 (0)	H(24)	4.4 (0)
H(3)	3.8 (0)	H(9A)	6.1 (0)	H(12C)	7.0 (0)	H(26)	3.8 (0)
H(4A)	6.2 (0)	H(9B)	6.1 (0)	H(14)	4.1 (0)	H(27)	4.2 (0)
H(4B)	6.2 (0)	H(9C)	6.1 (0)	H(15)	4.6 (0)	H(28)	4.2 (0)
H(5A)	6.4 (0)	H(10A)	5.3 (0)	H(16)	4.9 (0)	H(29)	4.5 (0)
H(5B)	6.4 (0)	H(10B)	5.3 (0)	H(17)	4.9 (0)	H(30)	3.8 (0)
H(6A)	5.7 (0)	H(10C)	5.3 (0)	H(18)	4.3 (0)	H(32)	3.9 (0)
H(6B)	5.7 (0)	H(11A)	6.5 (0)	H(20)	3.1 (0)	H(33)	4.8 (0)
H(6C)	5.7 (0)	H(11B)	6.5 (0)	H(21)	4.3 (0)	H(34)	5.7 (0)
H(7A)	6.8 (0)	H(11C)	6.5 (0)	H(22)	4.7 (0)	H(35)	5.5 (0)
H(7B)	6.8 (0)	H(12A)	7.0 (0)	H(23)	4.7 (0)	H(36)	4.5 (0)
H(8A)	6.3 (0)						

[a] The form of the anisotropic thermal ellipsoid is given by $\exp[-(B_{11}h^2 + B_{22}k^2 + B_{33}l^2 + 2B_{12}hk + 2B_{13}hl + 2B_{23}kl)]$. All hydrogen atoms were assigned isotropic thermal parameters as obtained for the atom bonded to the particular hydrogen atom.

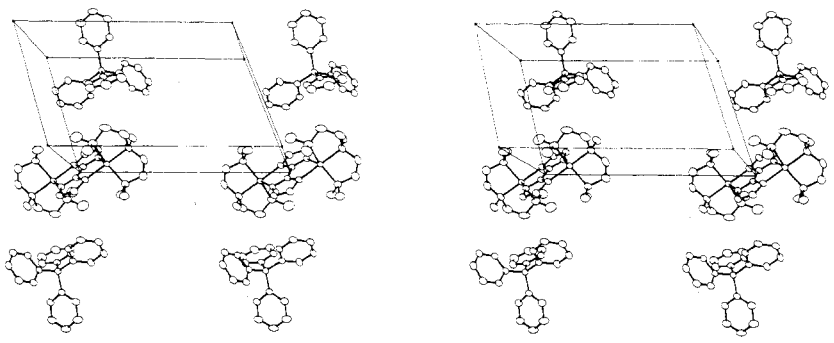

Figure 3. ORTEP plotting of the unit cell of $[Cu_2(Me_5dien)_2(BiIm)](BPh_4)_2$. Hydrogen atoms are not shown.

Table V. Principal Interatomic Distances (Å) and Angles (deg) for $[Cu_2(Me_5dien)_2(BiIm)](BPh_4)_2$

Distances within $[Cu_2(Me_5dien)_2(BiIm)]^{2+}$			
Cu-Cu′	5.489 (1)	N(3)-C(10)	1.484 (6)
Cu-N(1)	1.993 (3)	N(4)-C(5)	1.472 (7)
Cu-N(2)	2.324 (3)	N(4)-C(6)	1.485 (7)
Cu-N(3)	2.065 (3)	N(4)-C(7)	1.495 (7)
Cu-N(4)	2.024 (3)	N(5)-C(8)	1.479 (7)
Cu-N(5)	2.094 (3)	N(5)-C(11)	1.488 (7)
N(1)-C(1)	1.346 (4)	N(5)-C(12)	1.485 (8)
N(1)-C(2)	1.379 (4)	C(4)-C(5)	1.502 (10)
N(2)-C(3)	1.388 (5)	C(7)-C(8)	1.481 (8)
N(2)-C(1)′	1.325 (4)	C(2)-C(3)′	1.355 (5)
N(3)-C(4)	1.486 (6)	C(1)-C(1)′	1.449 (4)
N(3)-C(9)	1.472 (6)		
Angles within $[Cu_2(Me_5dien)_2(BiIm)]^{2+}$			
N(1)-Cu-N(2)	82.78 (10)	C(5)-N(4)-C(7)	112.4 (4)
N(1)-Cu-N(3)	94.92 (12)	C(5)-N(4)-Cu	106.9 (3)
N(1)-Cu-N(4)	174.10 (12)	C(6)-N(4)-C(7)	103.9 (4)
N(1)-Cu-N(5)	92.30 (12)	C(6)-N(4)-Cu	112.1 (3)
N(2)-Cu-N(3)	104.01 (11)	C(7)-N(4)-Cu	105.9 (3)
N(2)-Cu-N(4)	102.94 (12)	C(8)-N(5)-C(11)	111.8 (4)
N(2)-Cu-N(5)	99.91 (11)	C(8)-N(5)-C(12)	108.2 (4)
N(3)-Cu-N(4)	85.21 (13)	C(8)-N(5)-Cu	106.1 (3)
N(3)-Cu-N(5)	155.70 (13)	C(11)-N(5)-C(12)	109.5 (4)
N(4)-Cu-N(5)	85.29 (13)	C(11)-N(5)-Cu	107.1 (3)
C(1)-N(1)-C(2)	103.2 (3)	C(12)-N(5)-Cu	114.1 (3)
C(1)-N(1)-Cu	111.6 (2)	C(5)-C(4)-N(3)	109.4 (5)
C(2)-N(1)-Cu	144.9 (2)	N(4)-C(5)-C(4)	108.8 (5)
C(3)-N(2)-Cu	156.0 (2)	C(8)-C(7)-N(4)	109.4 (4)
C(4)-N(3)-C(9)	109.3 (4)	N(5)-C(8)-C(7)	109.5 (4)
C(4)-N(3)-C(10)	109.3 (4)	N(1)-C(2)-C(3)′	108.5 (3)
C(4)-N(3)-Cu	107.0 (3)	C(2)-C(3)′-N(2)′	109.9 (3)
C(9)-N(3)-C(10)	109.7 (4)	C(3)′-N(2)′-C(1)	102.5 (3)
C(9)-N(3)-Cu	112.7 (3)	N(1)-C(1)-N(2)′	116.0 (3)
C(10)-N(3)-Cu	108.7 (3)	N(1)-C(1)-C(1)′	120.8 (3)
C(5)-N(4)-C(6)	110.2 (4)	N(2)′-C(1)-C(1)′	123.2 (3)
Distances in the Tetraphenylborate Anion			
C(13)-C(14)	1.393 (5)	C(25)-C(26)	1.396 (5)
C(13)-C(18)	1.400 (5)	C(25)-C(30)	1.403 (5)
C(14)-C(15)	1.401 (6)	C(26)-C(27)	1.391 (5)
C(15)-C(16)	1.370 (6)	C(27)-C(28)	1.368 (6)
C(16)-C(17)	1.371 (6)	C(28)-C(29)	1.378 (6)
C(17)-C(18)	1.400 (6)	C(29)-C(30)	1.392 (5)
C(19)-C(20)	1.399 (5)	C(31)-C(32)	1.401 (5)
C(19)-C(24)	1.408 (5)	C(31)-C(36)	1.405 (5)
C(20)-C(21)	1.385 (5)	C(32)-C(33)	1.391 (6)
C(21)-C(22)	1.376 (5)	C(33)-C(34)	1.371 (7)
C(22)-C(23)	1.374 (6)	C(34)-C(35)	1.388 (7)
C(23)-C(24)	1.393 (5)	C(35)-C(36)	1.390 (7)
B-C(13)	1.663 (5)	B-C(25)	1.650 (5)
B-C(19)	1.651 (5)	B-C(31)	1.662 (5)
Angles in the Tetraphenylborate Anion			
C(14)-C(13)-C(18)	114.5 (3)	C(36)-C(31)-B	122.2 (3)
C(15)-C(14)-C(13)	123.7 (3)	C(26)-C(25)-C(30)	115.0 (3)
C(16)-C(15)-C(14)	119.4 (4)	C(27)-C(26)-C(25)	122.8 (3)
C(17)-C(16)-C(15)	119.4 (4)	C(28)-C(27)-C(26)	120.4 (4)
C(18)-C(17)-C(16)	120.4 (4)	C(29)-C(28)-C(27)	119.0 (4)
C(13)-C(18)-C(17)	122.6 (4)	C(30)-C(29)-C(28)	120.4 (4)
C(20)-C(19)-C(24)	113.9 (3)	C(25)-C(30)-C(29)	122.4 (3)
C(21)-C(20)-C(19)	123.4 (3)	C(32)-C(31)-C(36)	114.7 (3)
C(22)-C(21)-C(20)	120.7 (4)	C(33)-C(32)-C(31)	122.8 (4)
C(23)-C(22)-C(21)	118.3 (4)	C(34)-C(33)-C(32)	120.9 (4)
C(24)-C(23)-C(22)	120.6 (4)	C(35)-C(34)-C(33)	118.4 (5)
C(19)-C(24)-C(23)	123.0 (4)	C(36)-C(35)-C(34)	120.4 (4)
C(14)-C(13)-B	119.3 (3)	C(31)-C(36)-C(35)	122.8 (4)
C(18)-C(13)-B	126.2 (3)	C(13)-B-C(19)	113.4 (3)
C(20)-C(19)-B	122.7 (3)	C(13)-B-C(25)	106.5 (3)
C(24)-C(19)-B	123.4 (3)	C(13)-B-C(31)	107.4 (3)
C(26)-C(25)-B	121.8 (3)	C(19)-B-C(25)	106.9 (3)
C(30)-C(25)-B	122.7 (3)	C(19)-B-C(31)	110.5 (3)
C(32)-C(31)-B	123.0 (3)	C(25)-B-C(31)	112.1 (3)

N(3), N(4), and N(5). A stereoscopic view of the unit cell can be seen in Figure 3, and this shows how the large BPh_4^- ions isolate the $Cu_2(Me_5dien)_2(BiIm)^{2+}$ cations. The shortest interdimer Cu–Cu distance is 8.868 (1) Å, which is probably prohibitive of *inter*molecular magnetic exchange interactions.

Table VI. Least-Squares Planes for $[Cu_2(Me_5dien)_2(BiIm)]^{2+}$

atom	distance, Å	atom	distance, Å
Biimidazolate Plane[a]			
$0.570x + 0.899y - 0.1382z = 0.0$			
N(1)	−0.002 (3)	N(1)′	0.002 (3)
N(2)	0.001 (3)	N(2)′	−0.001 (3)
C(1)	0.001 (3)	C(1)′	−0.001 (3)
C(2)	0.003 (4)	C(2)′	−0.003 (4)
C(3)	−0.000 (4)	C(3)′	0.000 (4)
Square-Pyramid Plane Consisting of Atoms N(1), N(3), N(4), and N(5)[b]			
$0.7496x - 0.6521y - 0.1131z = -1.9064$			
N(1)	0.098 (3)	N(4)	0.188 (4)
N(3)	−0.152 (3)	N(5)	−0.175 (3)
Trigonal-Bipyramid Plane Consisting of Atoms N(2), N(3), N(5)[c]			
$-0.4118x + 0.0290y - 0.9108z = -1.8082$			
N(2)	0.000 (3)	N(5)	0.000 (3)
N(3)	0.000 (3)		

[a] The copper ions are 0.152 (4) Å out of this plane. [b] The copper ions are 0.2434 (4) Å out of this plane, and the N(2) atom is 2.520 (3) Å out of this plane. [c] The copper ions are 0.0655 (4) Å out of this plane.

Table VII

Least-Squares Planes for the Tetraphenylborate Phenyl Rings with Deviations and Estimated Errors

atom	distance, Å	atom	distance, Å
Plane 1: C(13), C(14), C(15), C(16), C(17), C(18)			
$-0.3897x + 0.8217y - 0.4158z = -0.1722$			
C(13)	0.000 (3)	C(16)	0.006 (4)
C(14)	0.008 (4)	C(17)	0.004 (5)
C(15)	−0.012 (4)	C(18)	−0.006 (4)
Plane 2: C(19), C(20), C(21), C(22), C(23), C(24)			
$-0.9533x + 0.2761y - 0.1224z = 4.1965$			
C(19)	−0.003 (3)	C(22)	−0.005 (4)
C(20)	0.001 (4)	C(23)	0.002 (5)
C(21)	0.003 (4)	C(24)	0.003 (4)
Plane 3: C(25), C(26), C(27), C(28), C(29), C(30)			
$-0.0091x - 0.5754y - 0.8178z = -6.3619$			
C(25)	0.014 (3)	C(28)	0.012 (4)
C(26)	−0.011 (3)	C(29)	−0.003 (4)
C(27)	−0.003 (4)	C(30)	−0.012 (4)
Plane 4: C(31), C(32), C(33), C(34), C(35), C(36)			
$-0.6811x - 0.7289y - 0.0696z = -6.8187$			
C(31)	−0.008 (3)	C(34)	−0.015 (5)
C(32)	0.008 (4)	C(35)	0.010 (5)
C(33)	0.002 (5)	C(36)	0.005 (4)

Dihedral Angles

ring A	ring B	∠AB, deg	ring A	ring B	∠AB, deg
1	2	49.5	2	3	93.9
1	3	97.9	2	4	62.8
1	4	107.7	3	4	62.0

All distances and angles in the BPh_4^- anion appear normal. The least-squares planes for the phenyl groups and the dihedral angles between planes are given in Table VII.

Magnetic Susceptibility and EPR. Variable-temperature (4.2–224 K) magnetic susceptibility data for $[Cu_2(Me_5dien)_2(BiIm)](BPh_4)_2$ were reported in a previous paper.[12] No indications of a magnetic exchange interaction were detected down to 4.2 K. In terms of an isotropic exchange Hamiltonian, $\hat{H} = -2J\hat{S}_1\cdot\hat{S}_2$, this means that $|J| <$ ca. 0.5 cm^{-1}. Figure 4 illustrates the liquid nitrogen temperature Q-band

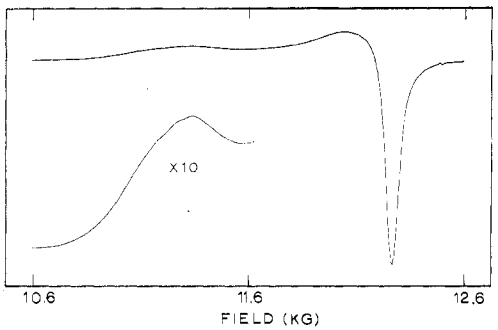

Figure 4. Liquid nitrogen temperature Q-band EPR spectrum of a powdered sample of $[Cu_2(Me_5dien)_2(BiIm)](BPh_4)_2$. Inset shows a 10× expansion of the $g_{||}$ signal.

EPR spectrum for this compound. Three signals are seen at $g = 2.208$, 2.084, and 2.041. The low-field signal with $g = 2.208$ is most likely the $g_{||}$ signal, which indicates that the electronic ground state of this complex is best viewed as distorted square pyramidal, i.e., $d_{x^2-y^2}$. The expanded view of the $g_{||}$ signal in Figure 4 shows that poorly resolved copper hyperfine splitting can be seen on this signal. The appearance of the hyperfine splitting is suggestive of the presence of an *intra*molecular magnetic exchange interaction in the binuclear cation.

The fact that the magnetic exchange interaction is so weak in $[Cu_2(Me_5dien)_2(BiIm)](BPh_4)_2$ can be explained in terms of the structure of the cation. Examination of either Figure 1 or Figure 2 shows that each imidazolate moiety of the $BiIm^{2-}$ unit bridges from an equatorial coordination site of one copper(II) complex to an axial site of the other copper(II) complex. Because the copper(II) complexes have $d_{x^2-y^2}$ ground states, only a very weak antiferromagnetic interaction would be expected as a consequence of the $BiIm^{2-}$ bridging into the axial site. The axial Cu–N(2) bond distance of 2.324 (2) Å would also lead to a weak interaction. The very weak coupling that is seen for $[Cu_2(Me_5dien)_2(BiIm)](BPh_4)_2$ is analogous to the case of oxalate-bridged $[Cu_2(dien)_2(Ox)](ClO_4)_2$. The X-ray structure[26] of this complex shows that the C–C bond distance for the Ox^{2-} bridge is essentially that of a single bond. If the Ox^{2-} bridge is to be considered as essentially two CO_2^- moieties coupled by a single C–C bond, then the analogy holds, for each CO_2^- moiety bridges between the two copper(II) complexes such that one oxygen atom bonds in an equatorial coordination site of one complex, whereas the second oxygen atom bonds in an axial site of the second complex. This complex also does not show any signs of a magnetic exchange interaction in susceptibility data taken down to 4.2 K.[27] Thus, the bis-bidentate construction of $BiIm^{2-}$ in $[Cu_2(Me_5dien)_2(BiIm)](BPh_4)_2$ places the two imidazolate moieties between two copper(II) ions in an orientation that does not lead to an appreciable exchange interaction.

It is interesting to compare the properties of the above $BiIm^{2-}$ complex with those of the analogous complex $[Cu_2(Me_5dien)_2(Im)](ClO_4)_3 \cdot H_2O$ prepared in this work. Figure 5 illustrates the magnetic susceptibility vs. temperature data obtained for this complex. The data are given in Table VIII.[16] As can be seen, there is a maximum in χ_M at 44 K, indicating the presence of an *intra*molecular antiferromagnetic exchange interaction propagated by the single Im^- bridge. The data were readily least-squares fit to the Bleaney–Bowers equation to give $J = -27$ cm^{-1} and $g = 2.075$. As can be seen in Figure 5, there is a small amount (1–2%) of a paramagnetic impurity as evidenced by the increase in χ_M at the low temperatures. A term of the form $(PAR)(4.2/T)$ was added to the Bleaney–Bowers equation to account for this impurity. PAR is the paramagnetic susceptibility of the impurity at 4.2 K, and this fits to a value of 0.0095 cgsu. This compound could be

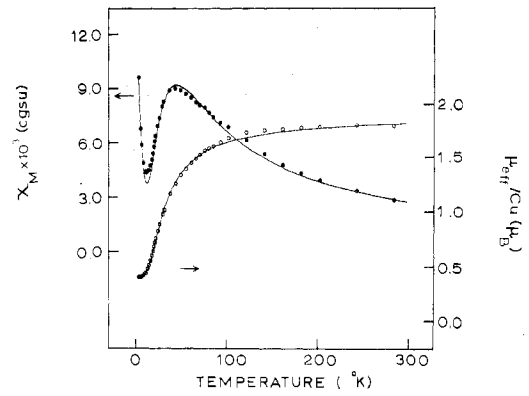

Figure 5. Molar paramagnetic susceptibility, χ_M, of the binuclear complex and effective magnetic moment per mole of copper(II) ion, μ_{eff}/Cu, vs. temperature curves for a solid sample of $[Cu_2(Me_5dien)_2(Im)](ClO_4)_3 \cdot H_2O$. The solid lines result from a least-squares fit of the data to the theoretical equation.

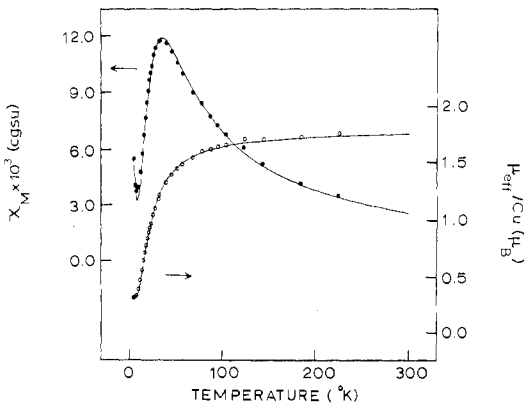

Figure 6. Molar paramagnetic susceptibility, χ_M, of the binuclear complex and effective magnetic moment per mole of copper(II) ion, μ_{eff}/Cu, vs. temperature curves for a solid sample of $[Cu_2(Et_5dien)_2(Im)](ClO_4)_3 \cdot 2H_2O$. The solid lines result from a least-squares fit of the data to the theoretical equation.

prepared in both the hydrated and anhydrous forms; both gave the same J values. The magnitude of the exchange interaction is essentially equal to that ($J = -25.80$ (16) cm^{-1}) recently reported by Lippard et al.[11] for $[(TMDT)_2Cu_2(Im)(ClO_4)_2](ClO_4)$, where TMDT is 1,1,7,7-tetramethyldiethylenetriamine. A single-crystal X-ray structure was obtained for the TMDT complex, and it showed that there is an imidazolate-bridged binuclear complex, $(TMDT)_2Cu_2(Im)(ClO_4)_2^+$, present in the compound. The copper(II) ions are five-coordinate by virtue of coordinating to the three TMDT nitrogen atoms, one nitrogen of the bridging imidazolate anion, and an oxygen atom of one ClO_4^-. The coordination geometry is square pyramidal with the oxygen of the perchlorate in the axial site. The plane of the Im^- is close to being perpendicular to the copper coordination planes.

The molecular structure of $[Cu_2(Me_5dien)_2(Im)](ClO_4)_3$ is most likely very similar to that found for $[(TMDT)_2Cu_2(Im)(ClO_4)_2](ClO_4)$ with the imidazolate bridging from one equatorial site to another equatorial site. It is clear, then, why the antiferromagnetic interaction observed for $[Cu_2(Me_5dien)_2(Im)](ClO_4)_3$ is so much greater than what was seen for $[Cu_2(Me_5dien)_2(BiIm)](BPh_4)_2$.

Three additional $[Cu_2(triamine)_2(Im)](ClO_4)_3$ compounds were prepared in this work to see if modifications of the triamine which are known to change the copper coordination geometry do affect the magnitude of the exchange interaction. Tables IX–XI[16] summarize the data obtained for $[Cu_2(Et_5dien)_2(Im)](ClO_4)_3 \cdot 2H_2O$, $[Cu_2(dien)_2(Im)](ClO_4)_3$, and

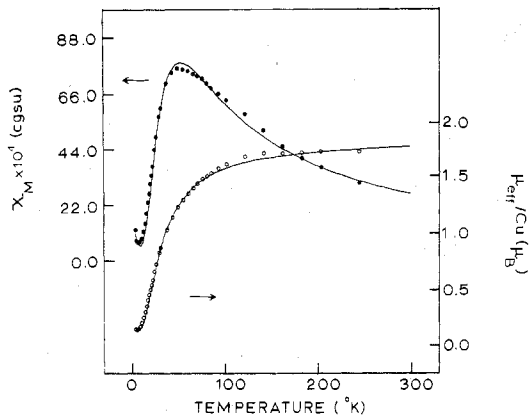

Figure 7. χ_M per mole of binuclear complex and μ_{eff} per mole of copper(II) ion vs. temperature curves for a solid sample of $[Cu_2(dien)_2(Im)](ClO_4)_3$. The solid lines result from a least-squares fit of the data to the theoretical equation.

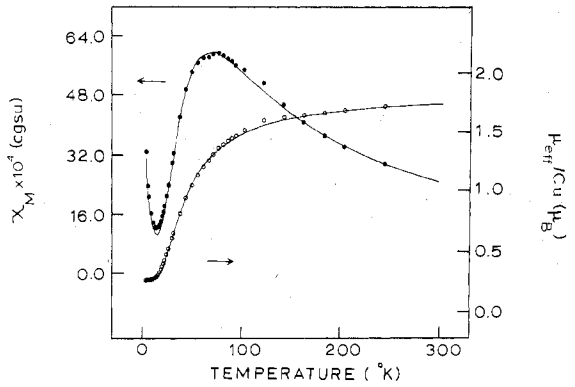

Figure 8. χ_M per mole of binuclear complex and μ_{eff} per mole of copper(II) ion vs. temperature curves for a solid sample of $[Cu_2(dpt)_2(Im)](ClO_4)_3$. The solid lines result from a least-squares fit of the data to the theoretical equation.

Table XII. Least-Squares Fitting Parameters for Magnetic Susceptibility Data[a]

compound	J, cm^{-1}	g	PAR, cgsu
$[Cu_2(Et_5dien)_2(Im)](ClO_4)_3 \cdot 2H_2O$	−20	2.038	0.0053
$[Cu_2(Me_5dien)_2(Im)](ClO_4)_3 \cdot H_2O$	−27	2.075	0.0095
$[Cu_2(dien)_2(Im)](ClO_4)_3$	−30	2.090	0.0010
$[Cu_2(dpt)_2(Im)](ClO_4)_3$	−39	2.056	0.0030

[a] The variable-temperature magnetic susceptibility data were least-squares fit to $\chi_M = (Ng^2\beta^2/kT)[2/(3 + \exp(-2J/kT))] + N\alpha + (PAR)(4.2/T)$. The temperature-independent paramagnetism, $N\alpha$, was set equal to 120×10^{-6} cgsu/mol of binuclear complex. PAR is the paramagnetic susceptibility of the monomeric impurity at 4.2 K. In the fitting procedure both J and g were varied.

$[Cu_2(dpt)_2(Im)](ClO_4)_3$, respectively. Figures 6–8 show that all three of these compounds also show antiferromagnetic interactions with peaks in their susceptibility vs. temperature curves at 32, 50, and 77 K, respectively. The susceptibility data for these three compounds were least-squares fit to give J values of −20, −30, and −39 cm^{-1}. Table XII lists all of the fitting parameters. It is clear, then, that changing the triamine ligand in these complexes does lead to a change in the magnitude of the antiferromagnetic exchange interaction, increasing in the order $Et_5dien < Me_5dien \simeq Me_4dien(TMDT) < dien < dpt$. The tendency of the antiferromagnetic interaction to increase in this order could be the result of several factors. If the local copper(II) ion coordination geometry is the same for each of the five complexes, then the increase in interaction could be a reflection of a change in the dihedral angle between the plane of the imidazolate bridge

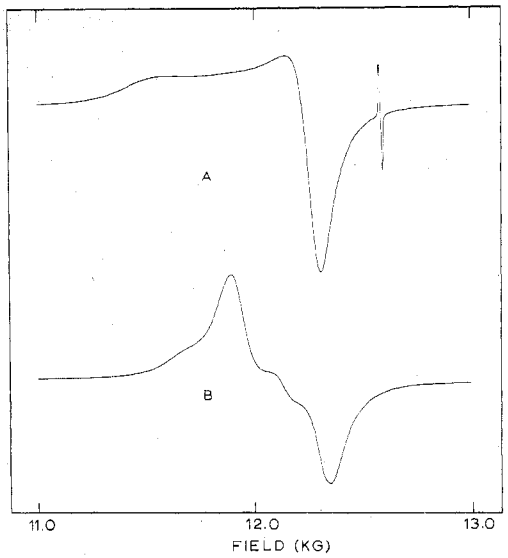

Figure 9. Liquid nitrogen temperature Q-band EPR spectra for powdered solid samples of (A) $[Cu_2(Me_5dien)_2(Im)](ClO_4)_3 \cdot H_2O$ and (B) $[Cu_2(dpt)_2(Im)](ClO_4)_3$.

and the basal planes of the square-pyramidal copper complexes. In the Me_4dien(TMDT) case, this angle is known[11] to be ca. 90°, perhaps due to the steric interactions between the methyl groups of Me_4dien and the Im^- bridge. These steric interactions would not be present in the dien and dpt complexes which could lead to a reduction in the dihedral angle. It is known[9,10] that when the Im^- bridge is coplanar with the basal planes of the copper coordination geometries, the interaction is greater with J = ca. −90 cm^{-1}.

One other possible explanation for the increased interaction in the dien and dpt complexes is that the local copper coordination geometry has changed from square pyramidal to a geometry that is closer to trigonal bipyramidal. It is known[12] that when the Im^- bridges from an axial site to another axial site in a binuclear copper(II) complex where the copper geometries are trigonal bipyramidal, the interaction is also increased. For example, for $[Cu_2(tren)_2(Im)](ClO_4)_3$, where tren is 2,2′,2″-triaminotriethylamine, J is −38 cm^{-1}.

Generally, EPR would have been expected to be useful in differentiating between the two above explanations for the change in exchange interaction by identifying whether any change in ground state is being experienced. Room-temperature and liquid nitrogen temperature X-band and Q-band EPR spectra were run for Et_5dien, Me_5dien, dien, and dpt imidazolate complexes. Figure 9 illustrates the Q-band EPR spectra for the Me_5dien and dpt complexes. At first it appeared to be startling how much the EPR spectra differed for these four compounds. Thus, the Q-band spectrum for the Et_5dien complex is an asymmetric single derivative centered at g = ca. 2.11, the Me_5dien and dien spectra show typical axial appearances with positions of apparent $g_\parallel$ and $g_\perp$ signals changed between the two, and the dpt spectrum seen in Figure 9 has a peculiar appearance. The complexity of some of these spectra and the variety can be understood when it is remembered that the presence of a single Im^- bridge gives a binuclear complex without a center of inversion. As a consequence, the **g** tensors at the two copper(II) ions in such a complex would be expected to be misaligned, producing potentially complicated spectra which could require a detailed analysis to infer the local copper(II) coordination geometries.

Acknowledgment. We are grateful for partial funding from National Institutes of Health Grant HL 13652. Thanks are also in order to Professor S. J. Lippard for sending us a preprint of ref 11. The X-ray diffraction equipment was

purchased in part by a departmental National Science Foundation grant. Dr. T. R. Felthouse is thanked for help with the ORTEP drawings.

Registry No. $[Cu_2(Me_5dien)_2(BiIm)](BPh_4)_2$, 66810-56-8; $[Cu_2(Et_5dien)_2(Im)](ClO_4)_3$, 68152-09-0; $[Cu_2(Me_5dien)_2(Im)](ClO_4)_3$, 68152-11-4; $[Cu_2(dien)_2(Im)](ClO_4)_3$, 68152-13-6; $[Cu_2(dpt)_2(Im)](ClO_4)_3$, 68152-15-8.

Supplementary Material Available: Tables I (analytical data) and VIII–XI (calculated and observed magnetic susceptibility data) and listings of observed and calculated structure factors (45 pages). Ordering information is given on any current masthead page.

References and Notes

(1) Part 18: C. G. Pierpont, L. C. Francesconi, and D. N. Hendrickson, *Inorg. Chem.*, in press.
(2) University of Illinois Fellow, 1976–1979.
(3) Camille and Henry Dreyfus Teacher–Scholar Fellowship, 1972–1977; A. P. Sloan Foundation Fellowship, 1976–1978.
(4) (a) J. S. Richardson, K. A. Thomas, B. H. Rubin, and D. C. Richardson, *Proc. Natl. Acad. Sci. U.S.A.*, **72**, 1349 (1975); (b) K. M. Beem, D. C. Richardson, and K. V. Rajagopalon, *Biochemistry*, **16**, 1930 (1977).
(5) J. A. Fee and R. G. Briggs, *Biochim. Biophys. Acta*, **400**, 439 (1975).
(6) (a) W. H. Vanneste, *Biochemistry*, **5**, 838 (1966); (b) G. Palmer, G. T. Babcock, and L. E. Vickery, *Proc. Natl. Acad. Sci. U.S.A.*, **73**, 2206 (1976).
(7) J. T. Landrum, C. A. Reed, K. Hatano, and W. R. Scheidt, *J. Am. Chem. Soc.*, **100**, 3232 (1978).
(8) M. F. Tweedle, L. J. Wilson, L. Garcia-Iniquez, G. T. Babcock, and G. Palmer, *Biochemistry*, in press.
(9) G. Kolks, C. R. Frihart, H. N. Rabinowitz, and S. J. Lippard, *J. Am. Chem. Soc.*, **98**, 5720 (1976).
(10) G. Kolks and S. J. Lippard, *J. Am. Chem. Soc.*, **99**, 5804 (1977).
(11) C.-L. O'Young, J. C. Dewan, H. R. Lilienthal, and S. J. Lippard, submitted for publication.
(12) M. S. Haddad and D. N. Hendrickson, *Inorg. Chem.*, **17**, 2622 (1978).
(13) S. W. Kaiser, R. B. Saillant, W. M. Butler, and P. G. Rassmussen, *Inorg. Chem.*, **15**, 2681 (1976).
(14) S. W. Kaiser, R. B. Saillant, W. M. Butler, and P. G. Rassmussen, *Inorg. Chem.*, **15**, 2688 (1976).
(15) B. F. Fieselmann, D. N. Hendrickson, and G. D. Stucky, *Inorg. Chem.*, **17**, 2078 (1978).
(16) Supplementary material.
(17) E. F. Hasty, L. Wilson, and D. N. Hendrickson, *Inorg. Chem.*, **17**, 1834 (1978).
(18) (a) B. N. Figgis and J. Lewis in "Modern Coordination Chemistry", J. Lewis and R. G. Wilkins, Eds., Interscience, New York, 1960, p 403; (b) P. W. Selwood, "Magnetochemistry", 2nd ed., Interscience, New York, 1956, pp 78, 92, 93.
(19) J. P. Chandler, Program 66, Quantum Chemistry Program Exchange, Indiana University, Bloomington, IN, 1973.
(20) All crystallographic calculations were carried out on the Syntex EXTL X-ray crystallographic package, based on the Data General ECLIPSE computer.
(21) "International Tables for X-Ray Crystallography", Vol. 2, J. A. Hiers and W. C. Hamilton, Eds., Kynoch Press, Burmingham, England, 1974, pp 99–102, 148, 150.
(22) D. T. Cromer and D. L. Liberman, *J. Chem. Phys.*, **53**, 1891 (1970).
(23) B. K. S. Lundberg, *Acta Chem. Scand.*, **26**, 3902 (1972).
(24) C. G. Pierpont, L. C. Francesconi, and D. N. Hendrickson, *Inorg. Chem.*, **16**, 2367 (1977).
(25) T. R. Felthouse and D. N. Hendrickson, *Inorg. Chem.*, **17**, 444 (1978).
(26) N. F. Curtis, I. R. N. McCormick, and T. N. Waters, *J. Chem. Soc., Dalton Trans.*, 1537 (1973).
(27) G. R. Hall, D. M. Duggan, and D. N. Hendrickson, *Inorg. Chem.*, **14**, 1956 (1975).

Contribution from the Istituto di Chimica Generale, Centro di Studio per la Strutturistica Diffrattometrica del C.N.R., University of Parma, 43100 Parma, Italy, Istituto di Chimica, Facoltà di Medicina-Veterinaria, University of Bari, 70126 Bari, Italy, and Istituto di Chimica Generale ed Inorganica, University of Modena, 41100 Modena, Italy

Halocuprates(II) of the *N*-Phenylpiperazinium Mono- and Dications: Crystal and Molecular Structure of *N*-Phenylpiperazinium Tetrachlorocuprate(II). Correlation of the Electronic Spectrum vs. Distortion of the $CuCl_4^{2-}$ Anions from Tetrahedral Symmetry

L. P. BATTAGLIA,[1a] A. BONAMARTINI CORRADI,[1a] G. MARCOTRIGIANO,[1b] L. MENABUE,[1c] and G. C. PELLACANI*[1c]

Received July 27, 1978

The X-ray structure of *N*-phenylpiperazinium tetrachlorocuprate(II), $(C_{10}H_{16}N_2)CuCl_4$, was determined by X-ray diffraction methods. Crystals are orthorhombic, $P2_12_12_1$, with $a = 17.698$ (2) Å, $b = 8.615$ (1) Å, $c = 9.841$ (1) Å, and $Z = 4$. A final R value of 4.3 was obtained. The structure consists of $[CuCl_4]^{2-}$ anions and *N*-phenylpiperazinium diprotonated cations. The $[CuCl_4]^{2-}$ anions show a flattened tetrahedral geometry, the two larger Cl–Cu–Cl angles being 141.1 and 143.0°; the dihedral angle is 51.6°. The Cu–Cl distances range from 2.23 to 2.27 Å. All four chlorine atoms are involved in Cl···N interactions, which may be responsible for the large distortion of the $[CuCl_4]^{2-}$ ion from the tetrahedral configuration. The *N*-phenylpiperazinium dication shows the usual "chair" configuration. The spectroscopic and magnetic results of the $[CuCl_4]^{2-}$ and $[CuCl_3Br]^{2-}$ anions are in agreement with a high distortion of these ions from tetrahedral symmetry. A study of the d–d transition maximum vs. the distortion of the $CuCl_4$ chromophore from the T_d symmetry is also reported. Some compounds containing the monoprotonated amine such as $(NPhpipzH)_2Cu_2X_6$ (X = Cl, Br) and $(NPhpipzH)_2Cu_2Cl_2Br_4$ are also studied. Their spectroscopic data suggest the presence of dimeric species in them with highly distorted tetrahedral symmetry.

Introduction

The halocuprate(II) and, in particular, the tetrachlorocuprate(II) anions have been extensively investigated for the great ease with which they assume various geometries, ranging from square planar through tetrahedral and on to trigonal bipyramidal.[2] The geometry of the $[CuX_4]^{2-}$ species in the solid state depends on many factors;[2] among them, the interactions due to crystal-packing forces and hydrogen bonding to cations are those on which the investigators may directly act.

Since cations like the piperidinium and morpholinium cations and the piperazinium dication have similar dimensions and therefore similar size effects, only the effect of the hydrogen bonding was recently investigated.[3,4]

In this paper the complexes formed between the *N*-phenylpiperazinium mono- and dication (hereafter abbreviated as NPhpipzH and $NPhpipzH_2$, respectively) and the copper halides are considered. This cation, which is bulkier than the piperazinium dication but preserves almost the same NH···X hydrogen-bonding ability, exerted between two metal–halogen layers, enabled us to extend our study to the size effects on the tetrahalocuprate(II) geometry.

Experimental Section

Preparation of the *N*-Phenylpiperazinium Hydrohalides. The *N*-phenylpiperazinium dihydrohalide salts were prepared by evaporating slowly and completely an aqueous amine solution neutralized

0020-1669/79/1318-0148$01.00/0